14th International Symposium on Turbulence and Shear Flow Phenomena (TSFP14)
Heidelberg, Germany, July 28–31, 2026

TWO-DIMENSIONAL TURBULENT CONDENSATES WITHOUT BOTTOM DRAG

Adrian van Kan
Institut für Geophysik,
Universität Münster
Correnstr. 24, 48149 Münster, Germany
avankan@uni-muenster.de

Alexandros Alexakis
Laboratoire de Physique de l'Ecole normale supérieure
ENS, Université PSL, CNRS, Sorbonne Université
24 rue Lhomond, 75005 Paris, France
alexandros.alexakis@phys.ens.fr

Edgar Knobloch
Department of Physics
University of California at Berkeley,
Berkeley, California, USA
knobloch@berkeley.edu

ABSTRACT

We use extensive direct numerical simulations of the incompressible two-dimensional (2D) Navier-Stokes equation to examine the steady state of large-scale condensates in 2D turbulence at finite Reynolds number Re in the absence of bottom drag. Large-scale condensates appear above a critical Reynolds number $Re_c \approx 4.19$. Close to this onset, we find a power-law scaling of the energy with $Re - Re_c$, where the energy spectrum at large scales follows the absolute equilibrium prediction of Kraichnan. At larger Re, the energy spectrum deviates from this form, displaying a steep power-law range at low wave numbers with exponent -5, with most of the energy dissipation occurring within the condensate at large scales. The spectral exponent is consistent with the logarithmic radial vorticity profile of the condensate vortices predicted by quasi-linear theory for a viscously saturated condensate. Our findings shed new light on the classical problem of large-scale turbulent condensation in forced dissipative 2D flows in finite domains, showing that the large scales are close to equilibrium dynamics in weakly turbulent flows but not in the strong condensate regime with $Re \gg 1$.

1 Introduction

Turbulence is a highly chaotic state of fluid flow at large Reynolds numbers (Frisch, 1995) that involves many degrees of freedom and therefore requires a statistical description. In this approach mean field quantities of interest should be derivable without detailed knowledge of the microscopic dynamics, much as the equation of state for a macroscopic system may be derived without detailed knowledge of individual molecular motions. However, approaches adapted from classical equilibrium statistical physics fail in general when applied to turbulence because the turbulent flow is typically far from thermodynamic equilibrium (Ruelle, 2012), with nonzero energy fluxes across scales and finite dissipation rates in the zero viscosity limit, both of which break time reversibility. Nevertheless, there are instances where the mean fluxes are negligible compared to fluctuations. This renders turbulence close to an equilibrium state, at least at certain scales, enabling equilibrium statistical physics approaches.

For 3D turbulence, Lee (1952) first applied equilibrium statistical physics to flows described by an ensemble of Fourier modes, arriving at a Rayleigh-Jeans spectrum $E(k) \propto k^2$. This work was later extended by Kraichnan, who incorporated the helicity constraint (Kraichnan, 1973). Lee's and Kraichnan's results strictly apply to the *truncated Euler equations* (Cichowlas *et al.*, 2005) (TEE) where a discrete set of wave numbers with finite modulus is retained in the evolution governed by the Euler equation of ideal (i.e., unforced and dissipationless) fluid flow, leading to a finite-dimensional dynamical system. However, these results apply in other instances as well. First, it has been argued theoretically (Forster *et al.*, 1977) and demonstrated (Dallas *et al.*, 2015; Alexakis *et al.*, 2023) that the Rayleigh-Jeans spectrum provides an adequate description of the scales above the forcing scale, with deviations from this spectrum studied by Hosking & Schekochihin (2023). Second, at the smallest scales of 3D turbulence, it has been argued (Frisch *et al.*, 2008) and recently shown numerically (Agrawal *et al.*, 2020) that when a high-order hyperviscosity is used the energy spectrum just above the hyperviscous scales forms a k^2 spectrum. Finally, when the Navier-Stokes equation is solved spectrally on a periodic domain in three dimensions, retaining a finite number of Fourier modes, it was shown in (Alexakis & Brachet, 2020) that, in the limit of small viscosity, the sharp spectral cutoff also leads to a k^2 spectrum, much like the effect of high-order hyperviscosity. In the latter two cases, the k^2 range forms due to an artificial block, also referred to as a bottleneck. This bottleneck makes the energy flux decrease abruptly at the largest available wave numbers k, producing near-equilibrium flow at these k.

In 2D turbulence, where energy is transferred towards larger scales (Boffetta & Ecke, 2012), there is a natural, and physically significant, smallest wave number in the system set by the inverse of the domain size. In the absence of an efficient large-scale dissipation mechanism, such as bottom drag, energy piles up at the largest scales, producing large-scale flow structures, also known as condensates (Sommeria, 1986). The weak dissipation and the reduced energy flux due to the low spectral cutoff both suggest that these scales might be described by equilibrium dynamics. The approach to describing such large-scale organisation in 2D fluid flows using equilibrium statistical physics goes back to Onsager (1949) who first analyzed 2D discrete point-vortex flows in terms of microcanonical statistical mechanics, revealing the existence of states with negative temperature, where point vortices of either sign cluster to form large-scale vortices. This line of work was further pursued, first for point vortices (Lundgren & Pointin,

1977) and later generalised to continuous vorticity fields obeying the 2D Euler equation in the so-called Robert-Sommeria-Miller theory (Robert & Sommeria, 1991; Miller *et al.*, 1992), which has been studied intensively (Bouchet & Venaille, 2012) with the goal of predicting the long-time evolution of turbulent large-scale structures.

In an alternative approach built on the *truncated* Euler equation, inspired by Lee's work in three dimensions, Kraichnan (Kraichnan, 1967) formulated an equilibrium theory for 2D turbulence. He assumed that the probability of a given state follows a Gibbs distribution familiar from canonical statistical mechanics, incorporating an additional ideal quadratic invariant, the enstrophy Ω (mean squared vorticity), together with the energy $\mathscr{E}$. This led him to predict the energy spectrum

$$E(k) = \frac{2\pi k}{\alpha + \beta k^2}, \tag{1}$$

where the constants α, β are generalised temperatures. These may be positive or negative. Their values are determined by total energy and enstrophy, $\mathscr{E} = \sum_{\mathbf{k}} E(k)$, and $\Omega = \sum_{\mathbf{k}} k^2 E(k)$, where the sum is over all wave numbers in the range $k_{min} \leq |\mathbf{k}| \leq k_{max}$, with the minimum wave number k_{min} (largest length scale) and the maximum wave number k_{max} (smallest length scale). In addition to Kraichnan's canonical ensemble, the statistical mechanics of the 2D TEE has also been studied microcanonically (Shukla *et al.*, 2016).

While Kraichnan's absolute equilibrium theory assumes that the statistics of the flow follow the TEE of ideal (unforced and dissipationless) fluid flow, it remains ill-understood how this relates to forced-dissipative turbulence. Early numerical studies investigated primarily the dynamics of freely decaying 2D turbulence (Brachet *et al.*, 1988; Weiss & McWilliams, 1993; Bracco *et al.*, 2000), in part due to limited available computational resources. Other work focused on the cascade phenomenology of forced 2D turbulence by introducing a strong bottom drag (also referred to as Rayleigh friction) that prevented the formation of a large-scale condensate, e.g. Boffetta (2007). The focus of many of the more recent numerical simulations, on the other hand, was on the forced-dissipative condensate state (Smith & Yakhot, 1993; Boffetta & Ecke, 2012; Frishman & Herbert, 2018; Xu *et al.*, 2024), where a well-defined statistically steady state is attained at late times. Chertkov *et al.* (2007) studied the transient dynamics of the build-up of the condensate under sustained forcing by integrating the 2D Navier-Stokes equation subject to periodic boundary conditions with small-scale stochastic forcing, hyperviscosity and no large-scale drag, producing (by construction) a transient simulation where energy kept increasing. Chertkov et al. reported a k^{-3} power-law range in $E(k)$ at small k associated with the large-scale condensate (a vortex dipole in physical space). However, the limitation of these results to the transient regime motivates the question of how this result is modified in a statistically stationary state where the condensate amplitude saturates due to dissipation at large scales. Such steady-state condensate states have been studied in recent years in the context of quasi-linear theory (Frishman, 2017), leveraging the strength of the mean flow compared to fluctuations to neglect nonlinear interactions between fluctuations except where they feed back on the mean flow. This theoretical work has led to explicit predictions for the profile of the large-scale condensate, with results that depend on the large-scale dissipation mechanism. When bottom drag saturates the condensate there is, at large Reynolds numbers, a range of radii with constant mean azimuthal velocity (Laurie *et al.*, 2014), while for a viscously saturated condensate one finds a mean azimuthal velocity profile of the form $r\ln(r/R)$ (Doludenko *et al.*, 2021), where r is the radial coordinate and R is the radius of the condensate, comparable to the domain size. These predicted spatial profiles have been confirmed in direct numerical simulations (DNS) when the condensate is strong.

Given the long history of statistical mechanics approaches to describing the condensate assuming an ideal fluid, it remains an open question whether the large scales in *forced dissipative* 2D turbulent condensates can in fact be described by equilibrium dynamics and, if so, under which conditions? We explore this question in detail, focusing on the case without bottom drag with condensates saturated viscously in the steady state. Our results indicate that close to the onset of 2D turbulence, where the upscale energy flux is small, the large scales display a Kraichnan equilibrium form in well-resolved DNS but only up to a finite Reynolds number *Re*. For larger *Re*, the condensate is far from equilibrium and quasi-linear theory applies, implying an energy spectrum close to k^{-5} at low k.

The remainder of this article is structured as follows. In Sec. 2 we describe our setup and discuss the relevant control parameters. In Sec. 3, we present our numerical results. Finally, in Sec. 4 we conclude with perspectives for future work.

2 Set-up

We consider incompressible flow in a 2D doubly periodic square domain of side length $2\pi L$, obeying

$$\partial_t \omega + \mathbf{u} \cdot \nabla \omega = \nu \nabla^2 \omega + f_\omega, \qquad \nabla \cdot \mathbf{u} = 0, \tag{2}$$

where $\mathbf{u} \equiv (u_x, u_y)$ is the velocity field, $\omega \equiv \partial_x u_y - \partial_y u_x$ is the vertical component of vorticity, ν is the fluid's kinematic viscosity and f_ω is the vertical component of the curl of an external body force. The forcing f_ω is composed of Fourier modes with wave vectors $\mathbf{k}$ lying in the isotropic ring $k_f \leq |\mathbf{k}| \leq k_f + \Delta k_f$ (where $\Delta k_f L = 4$), whose amplitudes evolve randomly, being δ-correlated in time, so that the energy injection rate is fixed to ε, while the enstrophy injection rate η is fixed to $\eta \simeq \varepsilon k_f^2$ (the equality here becomes exact when $\Delta k_f = 0$). The above system is characterised by only two non-dimensional numbers, namely, the Reynolds number based on the energy injection rate ε and the forcing scale k_f, viz. $Re \equiv \varepsilon^{1/3}/(k_f^{4/3}\nu)$, and the scale separation factor $\Lambda \equiv k_f L$ between the forcing scale and the domain size.

The incompressible vorticity equation is solved using the pseudo-spectral code GHOST (Mininni *et al.*, 2011) with a 2/3 de-aliasing rule and a second-order Runge-Kutta time advancement method on an evenly spaced spatial grid of size N in each direction. The finite resolution introduces a third non-dimensional number $k_{max}\eta$, where $k_{max} = N/(3L)$ is the maximum allowed wave number and $\eta \equiv \varepsilon^{-1/6} k_f^{-1/3} \nu^{1/2}$ is the enstrophy dissipation scale. For well-resolved runs $k_{max}\eta \gg 1$, which we ensure in all simulations. In the above set-up the smallest wave number k_{min} is such that $k_{min}L = 1$. The second smallest wave number is such that $|\mathbf{k}|L = \sqrt{2}$ which is significantly larger than k_{min} and may hamper comparison with predictions for the functional form of the spectrum in cases where a strong condensate forms such that $k_{min}^2 \gtrsim -\alpha/\beta$, where $\alpha < 0$ while $\beta > 0$. For this reason we also consider cases for which $k_{min}L > 1$, a situation achieved by artificially removing all wave numbers with $|\mathbf{k}|L < k_{min}L$ where $k_{min} \geq 1/L$ is chosen arbitrarily. This procedure allows us to reduce the spacing between the smallest and second smallest wave numbers, leading to a nearly continuous distribution of wave numbers and introducing a fourth non-dimensional number $\lambda = k_{min}L \geq 1$.

A large set of simulations was produced varying all four parameters. The scale separation Λ was varied between $\Lambda = 2$ and $\Lambda = 80$ while λ varied from $\lambda = 1$ to $\lambda = 10$. The

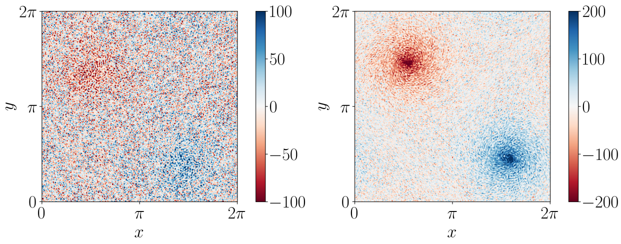

Figure 1. Vorticity field in the large-scale condensate in the statistically steady state with $\Lambda = 80$, $k_{min}L = 1$ and $Re = 4.32$ (left panel) and $Re = 7.25$ (right panel). Close to the onset of turbulence (left panel), the condensate is weak and diffuse, and barely visible relative to the sea of smaller-scale vortices. At larger Reynolds numbers (right panel) the condensate becomes sharply peaked within the cores of the counter-rotating large-scale vortices while the smaller-scale vortices in the interstitial space between them remain but are subdominant.

Reynolds number values achieved ranged from $Re \simeq 1$ to $Re \simeq 60$. The majority of the runs employed a resolution $N = 1024$ with $N = 512$ grid points used only for $Re < 4$ while grids with $N = 2048$ were used for the two highest values of Re examined in the $\Lambda \leq 40$ runs. The slow convergence in time to the statistically stationary state prevented us from examining larger values of Re with larger values of N. All runs were integrated until a statistically stationary state was reached, with the injection of kinetic energy balanced by viscous dissipation and all quantities fluctuating around a well-defined mean value.

3 Results

Here, we describe the results of our DNS in terms of steady-state energy, energy and enstrophy dissipation rates, spectra and fluxes, as well as the spatial profile of the vortices comprising the large-scale condensate. The physical space profile of the condensate is illustrated in Fig. 1 in terms of the vorticity field at two different Reynolds numbers $Re = 4.32$ (left, close to the onset of turbulence) and $Re = 7.25$ (right, strongly turbulent flow). While the condensate at $Re = 4.32$ is weak and barely visible in the vorticity field relative to the background of smaller-scale vortices, at $Re = 7.25$ a large-scale, large-amplitude vorticity dipole has clearly formed over the sea of smaller-scale vortices, which remain visible between the large-scale dipole. The purpose of this work is to describe this condensate state as a function of the parameters Re and Λ.

3.1 Global behaviour

Figure 2 shows the total kinetic energy $\mathscr{E} = \frac{1}{2}\langle|\mathbf{u}|^2\rangle$ of the flow (where $\langle\cdot\rangle$ is the space-time average) as a function of Re for all values of Λ and λ examined. Energy is scaled by $\varepsilon/(2\nu k_{min}^2)$ which collapses the data provided there is sufficient scale separation between the forcing scale and the largest scale in the domain, i.e., $\Lambda \gg 1$. Figure 2 shows that the only cases that escape this data collapse are those with small values of the scale separation factor Λ, viz. $\Lambda = 5$ and $\Lambda = 2$.

The behaviour of the energy as a function of Re constitutes a bifurcation diagram. For Re smaller than a critical value $Re_c \simeq 4.19$ the normalised energy assumes very small (albeit finite) values, while for $Re > Re_c$ the kinetic energy bifurcates towards order one magnitudes. The critical value Re_c depends weakly on the scale separation factor Λ but converges to a Λ-independent value as $\Lambda \to \infty$. This behaviour is consistent with a transition from positive to negative eddy viscosity $\nu_e(k) = \beta(Re) + \delta k^2 + \ldots$ (Dubrulle & Frisch, 1991), where the first term $\beta(Re)$ changes sign at Re_c. For $Re < Re_c$ the bifurcation is imperfect and the normalised energy is not zero,

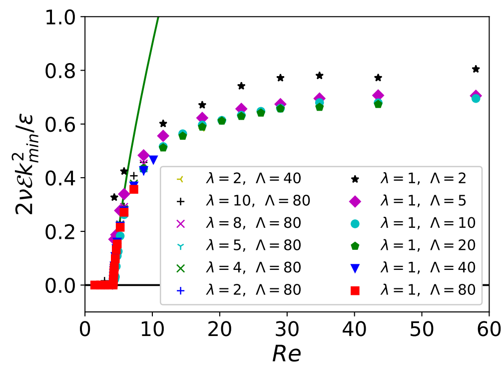

Figure 2. Energy bifurcation diagram. Energy normalised by $\varepsilon/\nu k_{min}^2$ over the range of Re examined for different values of the parameters λ and Λ. The green line shows a fit to the $\lambda \equiv k_{min}L = 1$, $\Lambda \equiv k_f L = 80$ data.

but as the scale separation Λ increases, it becomes smaller and smaller approaching a perfect bifurcation. For $Re > Re_c$, the energy amplitude follows a $(Re - Re_c)^\gamma$ power-law behaviour, where the exponent γ appears to be strictly smaller than one, with $\gamma \approx 0.75$. This exponent differs from what has been reported in past work with deterministic (Gallet & Young, 2013) and stochastic (Linkmann *et al.*, 2020) forcing. In Linkmann *et al.* (2020), which is closer to our work, γ was found to approach unity as the bottom drag is reduced. We stress, however, that computing critical exponents by a fitting procedure involves significant uncertainty; moreover, the forcing function considered by Linkmann et al. acts over a broader band of wave numbers than that considered here. For a one-dimensional deterministic bifurcation, one would expect $\gamma = 1$, but here the presence of noise as well as the fact that the large-scale energy is distributed among a set of wave numbers and not confined to a single mode may combine to lead to a different exponent.

We note that the energy satisfies the inequality $2\nu\mathscr{E}k_{min}^2/\varepsilon \leq 1$, a consequence of Poincaré's inequality $\langle|\nabla\mathbf{u}|^2\rangle \geq k_{min}^2\langle|\mathbf{u}|^2\rangle$. This bound is sharp when all the energy is concentrated in the $k = k_{min}$ modes. Our simulations show that this upper bound is missed by a substantial margin even at large values of Re. This fact indicates that the large-scale energy in steady state is proportional to $1/\nu$ and that the smaller scales retain a finite energy fraction even for $Re \to \infty$.

Steady-state energy and enstrophy balance gives

$$\varepsilon = \nu\Omega \quad \text{and} \quad \eta = \nu\mathscr{Z} \simeq \varepsilon k_f^2, \tag{3}$$

where $\Omega \equiv \langle|\nabla\mathbf{u}|^2\rangle$ is the enstrophy and $\mathscr{Z} \equiv \langle|\nabla\omega|^2\rangle$ is the palinstrophy. As $Re \to \infty$, $\Lambda \to \infty$, enstrophy is mostly dissipated in small scales while most of the energy is dissipated at large scales, reaching amplitudes $\mathscr{E} \propto \varepsilon/\nu k_{min}^2$. Without $\Lambda \to \infty$, a finite fraction of enstrophy dissipation occurs at large scales.

3.2 Spectra and Fluxes

To better understand the observed behaviour we plot in Fig. 3 the energy spectra for different values of Re and two values of the scale separation: $\Lambda \equiv k_f L = 80$ (top panel) which is the largest scale separation studied, and $\Lambda \equiv k_f L = 20$ (bottom panel) for which sufficiently large values of Re were reached to reveal the asymptotic behaviour of the energy (demonstrated in Fig. 2). Different stages in the form of the energy spectrum are observed as the Reynolds number varies. First, for very small Re, $Re \ll Re_c$, the dissipation dominates at all scales and the energy is concentrated at the forcing scale with a fast

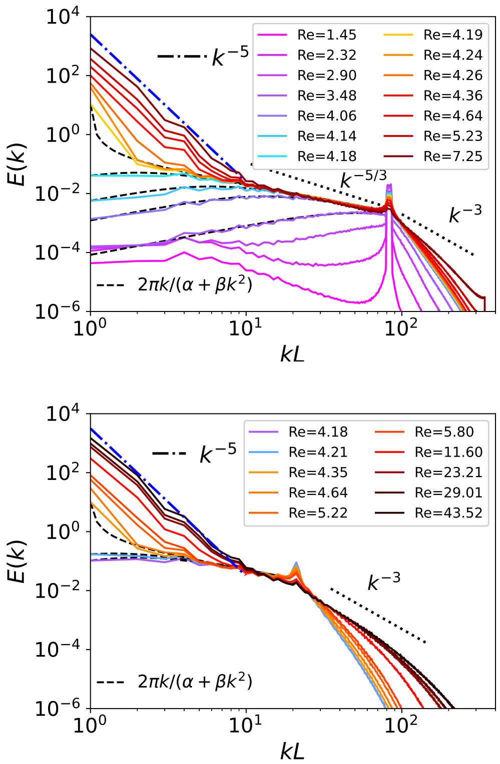

Figure 3. Energy spectra for the $k_{min} = 1$ runs with $\Lambda = 80$ (top) and $\Lambda = 20$ (bottom). The blue dashed-dotted line indicates the k^{-5} power law. Black dashed lines represent the best fit to the equilibrium spectra $E(k) = Ak/(k^2 - k_s^2)$, where A, k_s are fitting parameters and k_s can be imaginary (i.e., $k_s^2 < 0$).

exponential drop at larger wave numbers and a distribution at small wave numbers that is due to a "beating" effect from the forced modes. This beating is caused by pairs of forced modes with wave numbers that differ by Δk such that $|\Delta k| \ll k_f$ whose interaction due to nonlinearity then excites the small k modes (see appendix of Alexakis & Brachet (2019)). As Re increases, approaching Re_c from below, the dissipation at large scales remains negligible, while remaining significant for the forced modes. The spectrum in this regime attains a form that is very close to Kraichnan's absolute equilibrium prediction, cf. Eq. (1). This behaviour continues even after the threshold $Re = Re_c$ is crossed, leading to negative values of α/β, where α and β are the generalised temperature parameters obtained by fitting Kraichnan's spectrum to the DNS data. This observation supports the claim that the large-scale dynamics in 2D turbulence in the absence of large-scale friction can be described by equilibrium statistical physics for Re close to Re_c.

As Re is further increased and the condensate becomes stronger, the functional shape of the spectrum changes. A new k^{-5} power law appears (blue dash-dotted line), extending from the smallest wave number up to an intermediate wave number that increases as Re increases. In the bottom panel of Fig. 3, where $\Lambda = 20$ and larger values of Re are reached, the k^{-5} power law extends close to the forcing scale. As shown in the appendix of van Kan *et al.* (2025) and discussed below in Sec. 3.3, this steep k^{-5} power law at large scales is due to the formation of a condensate with a logarithmic vorticity profile that was recently predicted by Doludenko *et al.* (2021). For moderate Re the k^{-5} power-law is followed by a shallower power-law that is closer to the equilibrium prediction k^{-1} (dashed line) than to $k^{-5/3}$ (dotted line).

We remark that since energy is primarily dissipated at large scales $2\nu \int_{k_{min}}^{k_f} E(k)k^2 dk \approx \varepsilon$, and hence a spectrum of the form $E(k) = Ak^{-5}$ implies that the prefactor A at large Re becomes $A = \varepsilon k_{min}^2/\nu$. The blue dashed-dotted line in Fig. 3 compares this power-law with this prefactor with the corresponding result for the largest Re examined. Furthermore the fraction of enstrophy dissipation occurring at large scales, $\nu \int_{k_{min}}^{k_f} E(k)k^4 dk/\varepsilon k_f^2$, becomes proportional to $\Lambda^{-2}\ln(\Lambda)$, in agreement with our observation that enstrophy is dissipated primarily at small scales only when the scale separation factor $\Lambda \equiv k_f/k_{min}$ is sufficiently large. We emphasise finally that the k^{-5} profile depends on the form of the dissipation. If a weak bottom drag is considered instead, the vorticity profile becomes proportional to $1/r$ and the resulting spectrum in the statistically stationary state is k^{-3}, see e.g. Parfenyev (2024). The sensitivity to the type of dissipation reflects the fact that the condensate at high Re in this driven-dissipative setup is not a quasi-equilibrium state: as Re increases, the system transitions from a quasi-equilibrium to an out-of-equilibrium state.

The out-of-equilibrium nature of this system is associated with finite mean fluxes of energy and enstrophy across scales, shown in Fig. 4, averaged over the stationary state. The energy flux due to nonlinear interactions is given by $\Pi_E(K) = -\langle \mathbf{u}^{<K} \cdot (\mathbf{u} \cdot \nabla \mathbf{u}) \rangle$, where $\mathbf{u}^{<K}$ has been low-pass filtered to contain only Fourier modes with wave numbers of modulus less than K. The enstrophy flux is defined similarly as $\Pi_\Omega(K) = -\langle \omega^{<K} (\mathbf{u} \cdot \nabla \omega) \rangle$, where $\omega^{<K}$ is the low-pass-filtered vorticity. The energy flux Π_E becomes negative at scales larger than the forcing scale ($\Lambda \equiv k_f L = 80$ in the top panel, $\Lambda \equiv k_f L = 20$ in the bottom panel) as Re increases beyond Re_c, indicating an upscale energy transfer at a rate that increases with Re. There is a large variance in the energy flux at large Re, which leads to fluctuations that remain visible at low k and could only be further reduced by extensive averaging. The magnitude of the upscale flux approaches the energy injection rate ε as Re increases. The enstrophy, on the other hand, is transferred towards smaller scales at a rate that also increases with increasing Re. Here, the variance is smaller and the enstrophy flux approaches the enstrophy injection rate η at large Re. This positive enstrophy flux also drives wave numbers $k > k_f$ towards a k^{-3} spectrum at small scales as Re increases; see Fig. 3 and Boffetta & Musacchio (2010). We note that the constant inverse flux of energy and the constant forward flux of enstrophy demonstrated here is far from a trivial result in a system where no large scale dissipation mechanism is present and the system relies on viscous dissipation to saturate the large-scale energy growth. 2D turbulence only achieves this state by reaching sufficiently large condensate amplitude with a sufficiently steep spectrum so that all the energy injected is dissipated in just a few large-scale modes.

3.3 Radial vorticity Profile

The spectral viewpoint of the condensate state described above is complementary to a physical-space picture of the system. Recent investigations of the forced-dissipative condensate in the context of quasi-linear theory have led to explicit expressions for the spatial profile of the condensate vortices, with differing predictions depending on the dissipation mechanism saturating the growth of the condensate, as discussed earlier. In the present case of a viscously saturated condensate without bottom drag, Doludenko *et al.* (2021) predict a vorticity profile in the condensate state of the form

$$\overline{\omega}(r) = -2\Sigma(\log(r/L) + c_0), \qquad (4)$$

where $\overline{\omega}(r)$ is the time-averaged vorticity at distance r from the center of the condensate. The constant Σ has the dimen-

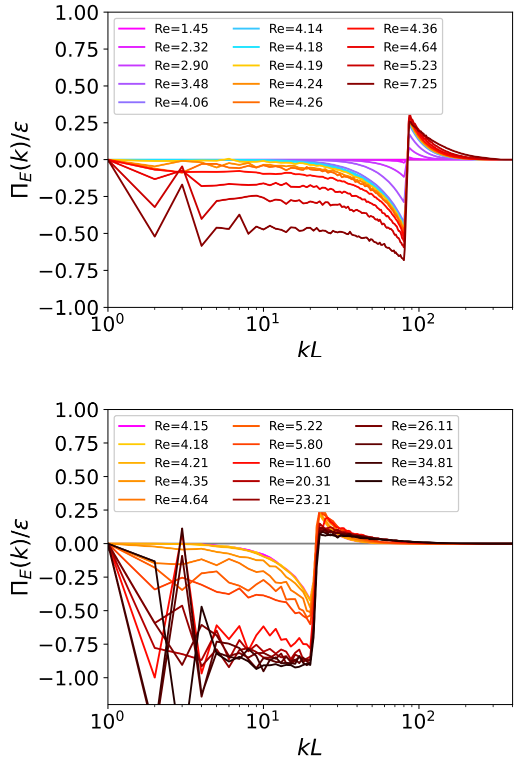

Figure 4. Energy flux for $\Lambda \equiv k_f L = 80$ (top), 20 (bottom) and different values of *Re*.

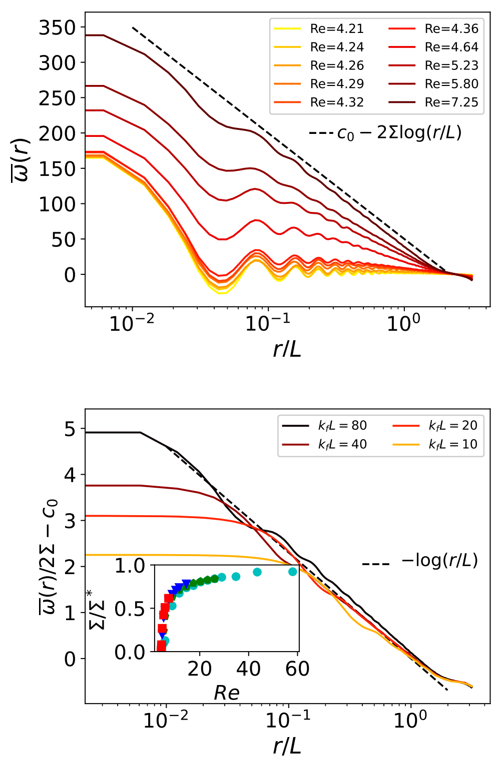

Figure 5. Top panel: Vorticity profile $\overline{\omega}(r)$ of the condensate for different *Re* (top) and $k_f L = 80$. The dashed line indicates the predicted functional form. Bottom panel: $\overline{\omega}(r)$ normalised by the measured quantity 2Σ for different values of $\Lambda \equiv k_f L$ (bottom) at the maximum value of *Re* reached. The inset shows the measured value of Σ normalised by $\Sigma^* \equiv \sqrt{\varepsilon/\nu}$.

sion of vorticity and in the $Re \to \infty$, $\Lambda \to \infty$ limit asymptotes to $\Sigma = \Sigma^* \equiv \pm\sqrt{\frac{\varepsilon}{\nu}}$, where the sign differs between the two counter-rotating large-scale vortices. Finally, c_0 is an order one constant. Expression (4) is valid for $1 \ll k_f r \ll k_f L$.

In Fig. 5 we plot the mean vorticity profile $\overline{\omega}(r)$ from different runs. To measure $\overline{\omega}(r)$ we trace for each instant of time the maximum and minimum value of the vorticity, and measure the mean vorticity at all grid points at distance r from these maxima. This procedure was repeated many times in the stationary state, and the time-averaged vorticity profile was calculated. The top panel displays the vorticity profile from the runs with the largest scale separation $k_f L = 80$. The bottom panel shows $\overline{\omega}(r)$ normalised by the measured 2Σ for different values of $\Lambda = k_f L$ and the largest *Re* attained at these Λ. For small *Re* spatial oscillations at the forcing scale are observed. As *Re* increases the amplitude around $r = 0$ increases and for sufficiently large $Re > Re_c$ the predicted functional form of $\overline{\omega}(r)$ is confirmed (top panel) and this is so over an increasingly wide range of radii at large *Re* as the scale separation factor Λ between the forcing scale and the domain size increases (bottom panel), in agreement with the prediction of Doludenko *et al.* (2021). The inset displays the measured value of the slope Σ normalised by Σ^*, showing that $\Sigma \approx \Sigma^*$ at large *Re*.

The spatial structure and the spectral properties of the condensate are naturally linked via the Fourier transform. In the appendix of van Kan *et al.* (2025), the Fourier transform of the logarithmic vorticity profile was computed, which yields an energy spectrum with a -5 exponent in agreement with the large-scale form of the energy spectra obtained in our DNS (Fig. 3). In contrast, when the condensate is saturated by a linear bottom drag, in which case the vorticity profile is of the form $\omega(r) \propto 1/r$, a k^{-3} spectrum is found instead, in agreement with the literature; see, e.g., Parfenyev (2024). It is interesting to note that the -3 exponent coincides with the value reported by Chertkov *et al.* (2007) for the case with no bottom drag or any other large-scale dissipation mechanism in their hyperviscous simulations. We surmise that these simulations were likely limited to the transient regime and failed to reach the final statistically stationary state. The agreement between the spectral exponents reported in the transient regime and the saturated condensate with bottom drag is thus coincidental since, as already discussed, the steady-state energy spectrum depends explicitly on the dissipation mechanism.

4 Conclusions

In this article we have characterised the viscously saturated condensate in stochastically forced 2D turbulence using extensive direct numerical simulations while varying independently both the Reynolds number *Re* and the scale separation Λ between the forcing scale and the domain size. The purpose of this work is to determine whether the condensate dynamics can be approximated by inviscid equilibrium theory or by quasi-linear theory wherein there is a local balance between energy injection and viscous dissipation. Our results establish that for sufficiently large scale separations, one or other of these two theories applies but over different ranges of *Re*.

When *Re* is close to its critical value for the onset of turbulence, large scales are well described by equilibrium dynamics. This is true both below and above onset. Above onset, a condensate forms but is predominantly composed of single-scale Fourier modes whose amplitude increases with *Re*. We emphasise that while the forcing-scale Reynolds number *Re* is of order one in this range, the effect of viscosity on the large scales is still negligible and so these scales are well described by inviscid dynamics. This becomes more and more so as the scale separation Λ increases. Close to the onset of turbulence at the critical Reynolds number $Re = Re_c \approx 4.19$, we find a self-similar scaling of the kinetic energy with $Re - Re_c$ with an exponent smaller than 1. The large-scale energy spectrum follows Kraichnan's equilibrium prediction for Re close to Re_c.

As Re increases further and the condensate becomes stronger, the energy spectrum deviates from this equilibrium form, showing a steep power-law range at low wave numbers with exponent -5. In this range of Re, most of the energy dissipation occurs within the condensate and so takes place at large scales supplied by a constant energy flux from the forcing scale to the largest scales of the system. In physical space, the condensate assumes a logarithmic profile in agreement with the quasi-linear theory prediction of Doludenko *et al.* (2021). We have shown that the spectral exponent -5 is a direct consequence of this logarithmic radial vorticity profile while the exponent -3 is found instead when the growth of the condensate is arrested by weak bottom drag. The deviations from the equilibrium predictions as well as the dependence of the condensate's functional form (in real and Fourier space) on the dissipation mechanism indicate that in the large Re limit, the large scales of forced-dissipative 2D turbulence are out-of-equilibrium and fit better with quasi-linear theory.

Several open questions for these viscously saturated condensates remain. The critical scaling exponent of the kinetic energy near the onset of 2D turbulence was only determined numerically and remains to be explained on theoretical grounds. Although this work focused on the case of two dimensions, the dependence of the results on the inclusion of a third dimension remains to be investigated, both in a quasi-2D setting (Alexakis, 2023; van Kan, 2024), for instance, in a thin-layer geometry (van Kan & Alexakis, 2019) or under the influence of rapid rotation (Seshasayanan & Alexakis, 2018) or topography (Siegelman & Young, 2023; Gallet, 2024), even though such studies will require significantly greater computational resources. Another important future direction is to examine the robustness of the results presented here for other forcing mechanisms and other forms of dissipation, e.g., linear or nonlinear bottom drag in the context of instability-driven turbulence (van Kan *et al.*, 2022), including turbulent convection (Guervilly *et al.*, 2014) and active turbulence (Alert *et al.*, 2022), where condensates can form (Linkmann *et al.*, 2019).

REFERENCES

Agrawal, Rahul, Alexakis, Alexandros, Brachet, Marc E & Tuckerman, Laurette S 2020 Turbulent cascade, bottleneck, and thermalized spectrum in hyperviscous flows. *Phys. Rev. Fluids* **5**, 024601.

Alert, Ricard, Casademunt, Jaume & Joanny, Jean-François 2022 Active turbulence. *Annu. Rev. Condens. Matter Phys.* **13**, 143–170.

Alexakis, Alexandros 2023 Quasi-two-dimensional turbulence. *Rev. Mod. Plasma Phys.* **7**, 31.

Alexakis, Alexandros & Brachet, Marc-Etienne 2019 On the thermal equilibrium state of large-scale flows. *J. Fluid Mech.* **872**, 594–625.

Alexakis, Alexandros & Brachet, Marc-Etienne 2020 Energy fluxes in quasi-equilibrium flows. *J. Fluid Mech.* **884**, A33.

Alexakis, Alexandros, Chibbaro, Sergio & Michel, Guillaume 2023 Fluctuation relations at large scales in three-dimensional hydrodynamic turbulence. *Europhys. Lett.* **144**, 43001.

Boffetta, Guido 2007 Energy and enstrophy fluxes in the double cascade of two-dimensional turbulence. *J. Fluid Mech.* **589**, 253–260.

Boffetta, G & Ecke, R E 2012 Two-dimensional turbulence. *Ann. Rev. Fluid Mech.* **44**, 427–451.

Boffetta, Guido & Musacchio, Stefano 2010 Evidence for the double cascade scenario in two-dimensional turbulence. *Phys. Rev. E* **82**, 016307.

Bouchet, Freddy & Venaille, Antoine 2012 Statistical mechanics of two-dimensional and geophysical flows. *Phys. Rep.* **515**, 227–295.

Bracco, A, McWilliams, J C, Murante, G, Provenzale, A & Weiss, J B 2000 Revisiting freely decaying two-dimensional turbulence at millennial resolution. *Phys. Fluids* **12**, 2931–2941.

Brachet, M E, Meneguzzi, M, Politano, H & Sulem, P L 1988 The dynamics of freely decaying two-dimensional turbulence. *J. Fluid Mech.* **194**, 333–349.

Chertkov, M, Connaughton, C, Kolokolov, I & Lebedev, V 2007 Dynamics of energy condensation in two-dimensional turbulence. *Phys. Rev. Lett.* **99**, 084501.

Cichowlas, Cyril, Bonaïti, Pauline, Debbasch, Fabrice & Brachet, Marc 2005 Effective dissipation and turbulence in spectrally truncated Euler flows. *Phys. Rev. Lett.* **95**, 264502.

Dallas, Vassilios, Fauve, Stephan & Alexakis, Alexandros 2015 Statistical equilibria of large scales in dissipative hydrodynamic turbulence. *Phys. Rev. Lett.* **115**, 204501.

Doludenko, A N, Fortova, S V, Kolokolov, I V & Lebedev, V V 2021 Coherent vortex in a spatially restricted two-dimensional turbulent flow in absence of bottom friction. *Phys. Fluids* **33**, 51–57.

Dubrulle, Bérengere & Frisch, Uriel 1991 Eddy viscosity of parity-invariant flow. *Phys. Rev. A* **43**, 5355–5364.

Forster, Dieter, Nelson, David R & Stephen, Michael J 1977 Large-distance and long-time properties of a randomly stirred fluid. *Phys. Rev. A* **16**, 732.

Frisch, Uriel 1995 *Turbulence: The Legacy of AN Kolmogorov*. CUP.

Frisch, Uriel, Kurien, Susan, Pandit, Rahul, Pauls, Walter, Ray, Samriddhi Sankar, Wirth, Achim & Zhu, Jian-Zhou 2008 Hyperviscosity, Galerkin truncation, and bottlenecks in turbulence. *Phys. Rev. Lett.* **101**, 144501.

Frishman, Anna 2017 The culmination of an inverse cascade: Mean flow and fluctuations. *Phys. Fluids* **29**, 125102.

Frishman, Anna & Herbert, Corentin 2018 Turbulence statistics in a two-dimensional vortex condensate. *Phys. Rev. Lett.* **120**, 204505.

Gallet, Basile 2024 Two-dimensional turbulence above topography: condensation transition and selection of minimum enstrophy solutions. *J. Fluid Mech.* **988**, A13.

Gallet, B & Young, W R 2013 A two-dimensional vortex condensate at high Reynolds number. *J. Fluid Mech.* **715**, 359–388.

Guervilly, Céline, Hughes, David W & Jones, Chris A 2014 Large-scale vortices in rapidly rotating Rayleigh–Bénard convection. *J. Fluid Mech.* **758**, 407–435.

Hosking, David N & Schekochihin, Alexander A 2023 Emergence of long-range correlations and thermal spectra in forced turbulence. *J. Fluid Mech.* **973**, A13.

van Kan, Adrian 2024 Phase transitions in anisotropic turbulence. *Chaos* **34**, 122103.

van Kan, A & Alexakis, A 2019 Condensates in thin-layer turbulence. *J. Fluid Mech.* **864**, 490–518.

van Kan, Adrian, Alexakis, Alexandros & Knobloch, Edgar 2025 Two-dimensional turbulent condensates without bottom drag .

van Kan, Adrian, Favier, Benjamin, Julien, Keith & Knobloch, Edgar 2022 Spontaneous suppression of inverse energy cascade in instability-driven 2-D turbulence. *J. Fluid Mech.* **952**, R4.

Kraichnan, Robert H 1967 Inertial ranges in two-dimensional turbulence. *Phys. Fluids* **10**, 1417–1423.

Kraichnan, Robert H 1973 Helical turbulence and absolute equilibrium. *J. Fluid Mech.* **59**, 745–752.

Laurie, Jason, Boffetta, Guido, Falkovich, Gregory, Kolokolov, Igor & Lebedev, Vladimir 2014 Universal profile of the vortex condensate in two-dimensional turbulence. *Phys. Rev. Lett.* **113**, 254503.

Lee, T D 1952 On some statistical properties of hydrodynamical and magneto-hydrodynamical fields. *Q. Appl. Math.* **10**, 69–74.

Linkmann, Moritz, Boffetta, Guido, Marchetti, M Cristina & Eckhardt, Bruno 2019 Phase transition to large scale coherent structures in two-dimensional active matter turbulence. *Phys. Rev. Lett.* **122**, 214503.

Linkmann, Moritz, Hohmann, Manuel & Eckhardt, Bruno 2020 Non-universal transitions to two-dimensional turbulence. *J. Fluid Mech.* **892**, A18.

Lundgren, T S & Pointin, Y B 1977 Statistical mechanics of two-dimensional vortices. *J. Stat. Phys.* **17**, 323–355.

Miller, Jonathan, Weichman, Peter B & Cross, M C 1992 Statistical mechanics, Euler's equation, and Jupiter's Red Spot. *Phys. Rev. A* **45**, 2328–2359.

Mininni, P D, Rosenberg, D, Reddy, R & Pouquet, A 2011 A hybrid MPI–OpenMP scheme for scalable parallel pseudospectral computations for fluid turbulence. *Parallel Comput.* **37**, 316–326.

Onsager, Lars 1949 Statistical hydrodynamics. *Il Nuovo Cimento (1943-1954)* **6**, 279–287.

Parfenyev, Vladimir 2024 Statistical analysis of vortex condensate motion in two-dimensional turbulence. *Phys. Fluids* **36**, 015148.

Robert, Raoul & Sommeria, Joel 1991 Statistical equilibrium states for two-dimensional flows. *J. Fluid Mech.* **229**, 291–310.

Ruelle, David P 2012 Hydrodynamic turbulence as a problem in nonequilibrium statistical mechanics. *Proc. Natl. Acad. Sci.* **109** (50), 20344–20346.

Seshasayanan, Kannabiran & Alexakis, Alexandros 2018 Condensates in rotating turbulent flows. *J. Fluid Mech.* **841**, 434–462.

Shukla, Vishwanath, Fauve, Stephan & Brachet, Marc 2016 Statistical theory of reversals in two-dimensional confined turbulent flows. *Phys. Rev. E* **94**, 061101.

Siegelman, Lia & Young, William R 2023 Two-dimensional turbulence above topography: Vortices and potential vorticity homogenization. *Proc. Natl. Acad. Sci. U. S. A.* **120** (44), e2308018120.

Smith, L M & Yakhot, V 1993 Bose condensation and small-scale structure generation in a random force driven 2D turbulence. *Phys. Rev. Lett.* **71**, 352–355.

Sommeria, Joël 1986 Experimental study of the two-dimensional inverse energy cascade in a square box. *J. Fluid Mech.* **170**, 139–168.

Weiss, Jeffrey B & McWilliams, James C 1993 Temporal scaling behavior of decaying two-dimensional turbulence. *Phys. Fluids A* **5**, 608–621.

Xu, Lichuan, van Kan, Adrian, Liu, Chang & Knobloch, Edgar 2024 Fluctuation-induced transitions in anisotropic two-dimensional turbulence. *Phys. Rev. Fluids* **9**, 064605.